

RAMAN SCATTERING SPECTRA AND DIELECTRIC RELAXATION BEHAVIOR OF PZT-PZN-PMnN CERAMICS

Le Dai Vuong¹ --- Phan Dinh Gio² --- Vo Thi Thanh Kieu³

¹Department of Physics, College of Sciences, Hue University and Faculty of Chemical and Environmental Engineering, Hue Industry College, Hue City, Vietnam

²Department of Physics, College of Sciences, Hue University, Vietnam

³Faculty of Chemical and Environmental Engineering, Hue Industry College, Hue City, Vietnam

ABSTRACT

The $0.8\text{Pb}(\text{Zr}_{0.48}\text{Ti}_{0.52})\text{O}_3-0.125\text{Pb}(\text{Zn}_{1/3}\text{Nb}_{2/3})\text{O}_3-0.075\text{Pb}(\text{Mn}_{1/3}\text{Nb}_{2/3})\text{O}_3 + 0.7 \text{ wt\% Li}_2\text{CO}_3 + 0.3 \text{ wt\% Fe}_2\text{O}_3$ ceramics (PZT-PZN-PMnN) have been prepared by two-stage calcination method. The influences of sintering temperature on dielectric properties and Raman scattering in the PZT-PZN-PMnN relaxor ferroelectric ceramics have been investigated in detail. The dielectric studies showed that the degree of diffuseness (γ) increased with the increase of the sintering temperatures from 900 to 1000 °C, indicating that the dielectric relaxation behavior was increased; while at higher sintering temperature above 1000 °C, the γ decreased. The dielectric measurement results are in good agreement with the Raman scattering spectra analysis of the samples. It was found that the value of full wide of half maximum (FWHM) of silent B_1+E mode reached the maximum value at the sintering temperature of 1000 °C, which showed similar trends to γ . At sintering temperature of 1000 °C, the highest dielectric constant (ϵ_{max}) of 23600 and the γ value of 1.84.

Keywords: Piezoelectric, Fe_2O_3 doping, EDS spectrum, Raman scattering.

1. INTRODUCTION

Relaxor ferroelectric materials have the high dielectric constant, broad ferroelectric-paraelectric transition (the diffuse phase transition) and strong frequency dependence of dielectric properties [1,2]. So far, researchers have been interesting on the Pb-based relaxors $\text{Pb}(\text{B}'_{1/3}\text{B}''_{2/3})\text{O}_3$ because they are promising materials for multilayer capacitors, transducer and actuators [2-6].

The addition of small amounts of such relaxor materials was found to be beneficial for the electrical properties of PZT-based ceramics due to the formation of fine and uniform rhombohedral domains along tetragonal ones [4,7]. Recently, it was observed that both the dielectric and piezoelectric properties of these PZT-relaxor materials are strongly influenced by the addition of other additives such as La_2O_3 , ZnO, CuO, MnO_2 and Fe_2O_3 [2, 4, 8]. The Fe_2O_3

addition is probably one of the most frequently used acceptors in ferroelectrics. The effects of Fe_2O_3 on PZT and PZT-based ternary ceramics have been studied [9-12]. However, the effect of Fe_2O_3 addition on the quaternary PZT-PZN-PMnN was scarcely reported.

Raman scattering spectrum analysis is an effective and qualitative method in studies of the microstructure of materials, especially when microscopic features such as atomic bonds and polarization are involved [10, 13, 14]. Raman investigation of ferroelectrics was first carried out in ferroelectric single-crystal specimens, for example, BaTiO_3 and PbTiO_3 [14-16] because polarization features of lattice vibration can be determined. For ceramics, Burns and Scott [17] measured and interpreted the Raman scattering spectrum of PZT ceramics 40 years ago. Their results showed that the frequency peaks in Raman spectra of ceramic corresponded well to the normal modes in single crystals. Since then, Raman scattering spectra from the ferroelectric ceramics have been widely used to investigate the phase structure.

In this paper, the influences of sintering temperature on dielectric properties and Raman scattering in the relaxor ferroelectric PZT-PZN-PMnN have been investigated in detail.

2. EXPERIMENTAL PROCEDURE

The general formula of the studied material was $0.8\text{Pb}(\text{Zr}_{0.48}\text{Ti}_{0.52})\text{O}_3 - 0.125\text{Pb}(\text{Zn}_{1/3}\text{Nb}_{2/3})\text{O}_3 - 0.075\text{Pb}(\text{Mn}_{1/3}\text{Nb}_{2/3})\text{O}_3 + 0.7 \text{ wt}\% \text{Li}_2\text{CO}_3 + 0.3 \text{ wt}\% \text{Fe}_2\text{O}_3$ (PZT-PZN-PMnN). Reagent grade oxide powders (purity $\geq 99\%$) of PbO , ZnO , MnO_2 , Nb_2O_5 , ZrO_2 , TiO_2 , Li_2CO_3 and Fe_2O_3 were used as starting materials. Firstly, the powders of $(\text{Zn,Mn,Fe})\text{Nb}_2(\text{Zr,Ti})\text{O}_6$ were prepared by reactions of ZnO , MnO_2 , Nb_2O_5 , ZrO_2 , TiO_2 and Fe_2O_3 at temperature $1100\text{ }^\circ\text{C}$ for 2 h. Then $(\text{Zn,Mn,Fe})\text{Nb}_2(\text{Zr,Ti})\text{O}_6$ and PbO were weighed and milled for 8 h. The powders were calcined at temperature $850\text{ }^\circ\text{C}$ for 2 h, producing the PZT-PZN-PMnN compound. Thereafter, predetermined amounts of Li_2CO_3 were mixed with the calcined PZT-PZN-PMnN powder, and then, powders milled for 16h. The ground materials were pressed into disk 12mm in diameter and 1.5mm in thick under 100MPa. The samples were sintered at 900, 950, 1000, and 1050 $^\circ\text{C}$ for 2 h (M1, M2, M3, M4).

The ceramic samples were poled in a silicone oil bath at $120\text{ }^\circ\text{C}$ by applying the DC electric field of 30 kVcm^{-1} for 20 min then cooling down to room temperature (RT). They were aged for 24 h prior to testing. Raman scattering spectra were recorded from a Raman Spectrometer (Jobin-Yvon Inc., Paris, France) using a backscattering configuration; the excitation laser was irradiated from an Ar^+ laser with a wavelength of 488 nm and output power of 11 mW. Energy dispersive spectra (EDS) were measured using a Hitachi S-3400 N scanning electron microscope with an EDS system Thermo Noran.

3. RESULTS AND DISCUSSION

3.1. Analysis of the Chemical Composition of Ceramics

In order to determine chemical composition of the PZT-PZN-PMnN ceramics, the EDS spectrum is analyzed and shown in Fig. 1. From Fig. 1 shows the presence of Pb, Zr, Ti, Nb, Zn, Mn and Fe elements whose weigh percentages shown in Tabe. 1. However, the EDS spectrum of

ceramic sample could not show the presence of lithium (Li) because of its atomic number is low and the mass percentage is too small [18].

Fig-1. EDS spectrum of PZT–PZN–PMnN ceramics

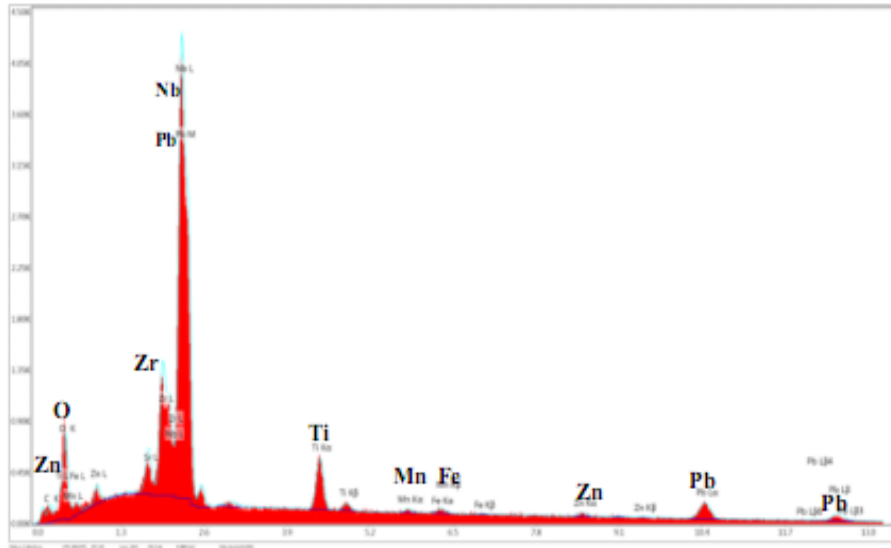


Table 1 shows the comparison in mass of Pb, Zr, Ti, Nb, Zn, Mn and Fe elements before and after sintering of the PZT-PZN-PMnN ceramics. It is quite clearly that the chemical composition of the synthesized ceramics can roughly accord with the general formula of the material.

Table-1. Chemical composition of the Fe₂O₃-doped PZT–PZN–PMnN ceramics

Elements	Mass percentage of elements from the precursors	Mass percentage of elements from the synthesized ceramics
Pb	64.4	59
Zr	10.72	10.13
Ti	6.10	5.19
Nb	3.79	3.06
Zn	0.83	0.59
Mn	0.42	0.43
Fe	0.09	0.10

3.2. Analysis of Raman Scattering Spectra of Ceramics

Fig. 2 and Fig. 3 show the Raman scattering spectra of PZT–PZN–PMnN ceramics measured at room temperature. As can be seen from Fig. 2 and Fig. 3, two wide bands of 140–400 and 400–900 cm⁻¹, respectively, can be observed in the measured range 100–1000 cm⁻¹. Compared with PZT, the vibration bands in the Raman scattering spectra of PZT–PZN–PMnN samples seem wider and more dispersive. As reported in the literature [1-3, 5, 8, 13], PZN and PMnN are typical relaxor ferroelectrics with a perovskite structure belonging to an R3m symmetry, similar to the rhombohedral PZT. The formation of PZT–PZN–PMnN solution enhances the disorder in

B site ions, which may result in the widening of the Raman bands. This is in good accordance with the measurement of dielectric constant ϵ versus temperature. It will be discussed in section 3.3.

According to the factor group analysis the PZT has 12 optical normal modes of symmetry $\Gamma = 4E + 3A_1 + B_1$ that are Raman modes [8, 13, 19]. In the studied frequency region, the major Raman shift peaks located at around 140, 205, 270, 330, 430, 580, 680, 740, and 825 cm^{-1} can be well fitted to nine vibration modes of $A_1(1\text{TO})$, $E(2\text{TO}_1)$, silent ($E+B_1$), $A_1(2\text{TO})$, $E(2\text{LO})$, R_1 , $E(4\text{LO})$, R_h and $A_1(3\text{LO})$ (Fig. 3), respectively [4, 8, 13, 14, 17, 19]. According to the results in other perovskiteniobates [13] these lines are assigned to the A site (Pb) stretching modes at 140 cm^{-1} , the O–B–O bonding modes at 205–270 cm^{-1} , the Zn–O–Zn bonds at 430 cm^{-1} , the Nb–O–Nb bonds at 580 cm^{-1} , the stretching mode of Nb–O–Zn bonds at 680 cm^{-1} , and the stretching mode of Nb–O–Fe bonds at 825 cm^{-1} . Fig. 4 shows the dependence of the Raman shifts of the five modes of PZT–PZN–PMnN samples. As seen from Fig. 4, the silent B_1+E mode shifted toward the higher frequencies with increase sintering temperature. The shift of the silent mode to a high frequency due to sintering temperature increases the average energy of the B–O bonding because the silent mode results from the vibration of centered ions of the octahedron. This is in good accordance with the measurement of Curie temperature. The relationships between Raman scattering spectra and dielectric properties of ceramics are discussed in the next section.

Fig-2. The Raman scattering spectra of PZT–PZN–PMnN ceramics with different sintering temperatures

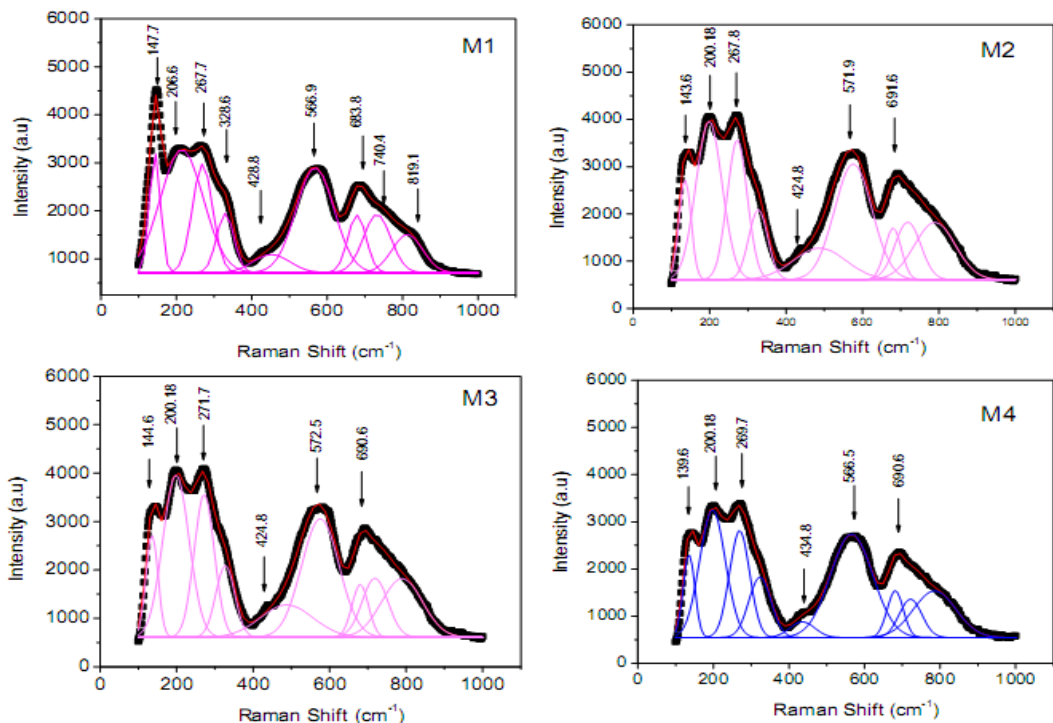


Fig-3. The major Raman shift peaks located at different frequencies of M1, M1, M3 and M4 samples

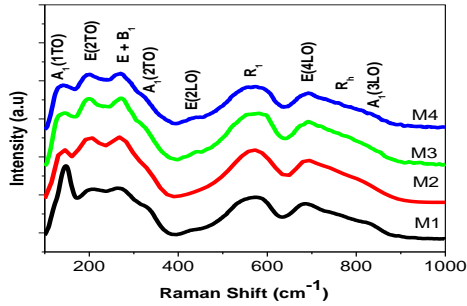
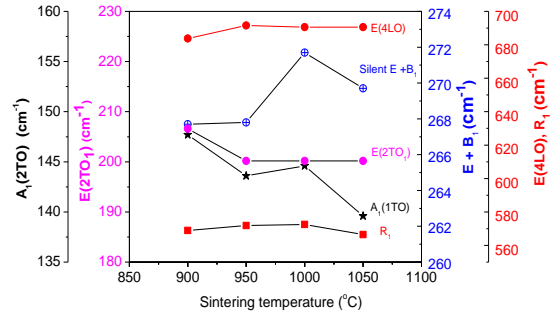


Fig-4. Raman shifts of the different modes of samples as a function of sintering temperatures



3.3. Dielectric Properties of Ceramics

Fig-5. Temperature dependence of the dielectric constant and dielectric loss $\tan\delta$ at 1 kHz frequency of ceramic samples

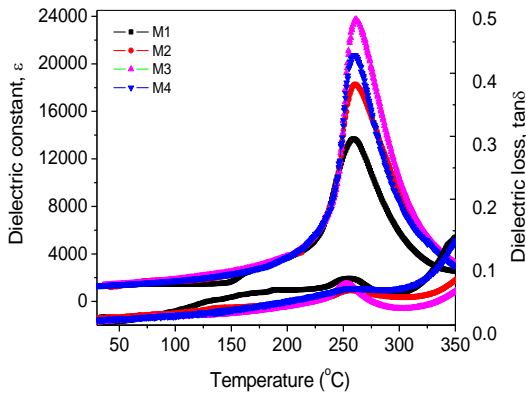


Fig-6. The T_m temperature of PZT-PZN-PMnN ceramics with different sintering temperature

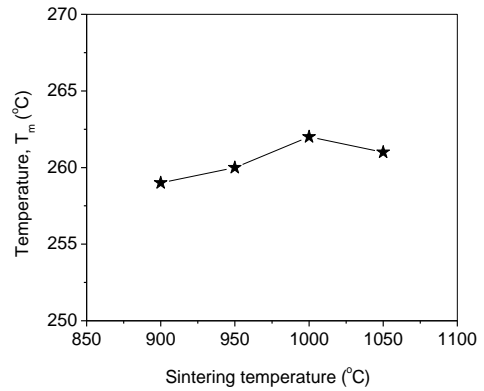


Fig-7. $\ln(1/\epsilon - 1/\epsilon_{max})$ as a function of $\ln(T - T_{max})$ at 1 kHz for samples

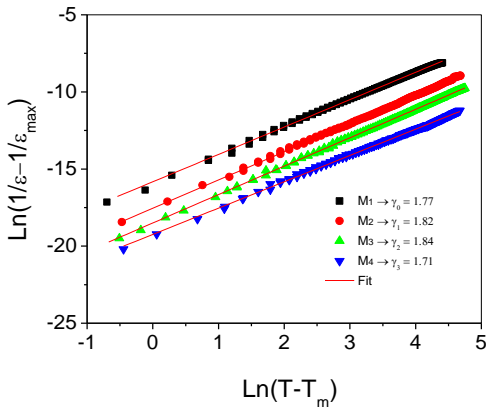
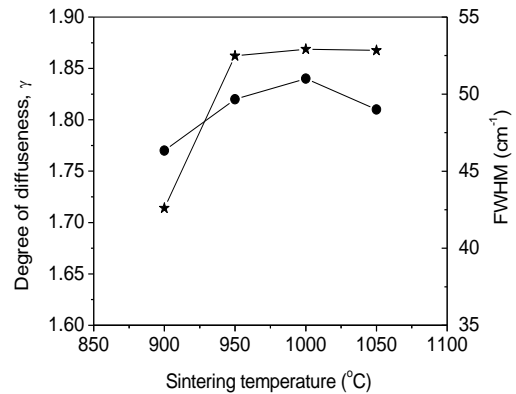


Fig-8. The degree of diffuseness γ and FWHM of the PZT-PZN-PMnN samples



The change of sintering temperature also significantly affects on dielectric properties of PZT–PZN–PMnN ceramics. Fig. 5 shows the dependence of dielectric constant ϵ and dielectric loss $\tan\delta$ of the ceramics versus temperature at 1 kHz. As observed, the dielectric properties exhibited characteristics of a relaxor material in which the phase transition temperature occurs within a broad temperature range. This result is good agreement with the studied Raman scattering spectra of the samples (the widening of the Raman bands). The maximum dielectric constant (ϵ_{\max}) increases with increasing sintering temperature, and at 1000 °C, the highest dielectric constant ϵ_{\max} of about 23600. However, with further increase in sintering temperature over 1000 °C, ϵ_{\max} decreased, which may be due to the creation of Pb vacancies.

From the results in Fig. 5, the temperature of the maximum dielectric constant (T_m) of the ceramic samples are determined (Fig 6). Corresponding sintering temperature increases from 900 to 1000 °C, T_m temperature of ceramics increased lightly from 259 to 262 °C and then sharply decreases beyond this point. As mentioned above, the silent B_1+E mode shifted toward the higher frequencies with increase sintering temperature. The shift of the silent mode to a high frequency due to sintering temperature increases the average energy of the B–O bonding hence T_m of the ceramics are increased.

To describe the diffuseness of phase transition for this composition, we use a modified empirical expression proposed by Uchino and Nomura [20].

$$\frac{1}{\epsilon} - \frac{1}{\epsilon_{\max}} = \frac{(T - T_m)^\gamma}{C} \quad (1)$$

where, ϵ_{\max} is the maximum value of dielectric constant at the phase transition temperature T_m , γ is the degree of diffuseness, and C is the Curie-like constant. γ has value ranging from 1 (normal ferroelectric) to 2 (ideal relaxor ferroelectric). The plot of $\ln(1/\epsilon - 1/\epsilon_{\max})$ versus $\ln(T - T_m)$ of ceramics at 1 kHz is shown in Fig. 7. The slopes of the fitting curves (Eq.1) are used to determine the γ value. The value of γ gives information on the phase transition diffuse character. The values of $\gamma = 1.77, 1.82, 1.84$ and 1.71 for M1, M2, M3 and M4 samples, respectively. It is clear that the value of γ increases with increase of sintering temperature (Fig. 8). The phase transition becomes more diffuse when the sintering temperature increases. This is linked to the increase of disorder in the ceramics. These results are in good agreement with the studied Raman scattering spectra of the samples. As can be seen in Fig. 8, when the sintering temperature of ceramics is lower than 1000 °C the silent B_1+E mode full width at half maximum (FWHM) increases with increasing sintering temperature. It is found that the FWHM of the B–O vibrations exhibit an obvious increase, leading to a strong composition disorder. However, with the sintering temperature is higher than 1000 °C, the value of γ and FWHM decreases. The decrease γ and FWHM of the samples sintered higher than 1000 °C may be caused by the evaporation of the PbO during the sintering at higher temperature.

4. CONCLUSIONS

Raman scattering spectroscopy and dielectric properties of $0.8\text{Pb}(\text{Zr}_{0.48}\text{Ti}_{0.52})\text{O}_3 - 0.125\text{Pb}(\text{Zn}_{1/3}\text{Nb}_{2/3})\text{O}_3 - 0.075\text{Pb}(\text{Mn}_{1/3}\text{Nb}_{2/3})\text{O}_3 + 0.3\text{wt}\%\text{Fe}_2\text{O}_3$ (PZT-PZN-PMnN) ceramics

sintered at different temperatures from 900 to 1050 °C were studied. In the studied frequency region, the major Raman shift peaks located at around 140, 205, 270, 330, 430, 580, 680, 740, and 825 cm^{-1} can be well fitted to nine vibration modes of $A_1(1\text{TO})$, $E(2\text{TO}_1)$, silent ($E+B_1$), $A_1(2\text{TO})$, $E(2\text{LO})$, R_1 , $E(4\text{LO})$, R_h and $A_1(3\text{LO})$.

The dielectric properties measurement results of ceramics are in good agreement with the studied Raman analysis of the samples. It was found that the value of full wide of half maximum (FWHM) of silent B_1+E mode reached the maximum value at the sintering temperature of 1000°C, which showed similar trends to γ . At sintering temperature of 1000 °C, the highest dielectric constant (ϵ_{max}) of 23600 and the γ value of 1.84.

REFERENCES

- [1] H. Fan and H. Kim, "Perovskite stabilization and electromechanical properties of polycrystalline lead zinc niobate–lead zirconate titanate," *Journal of Applied Physics*, vol. 91, pp. 317-322, 2002.
- [2] Y. Xu, *Ferroelectric materials and their applications*. Amsterdam-London-Newyork-Tokyo: North-Holland, 1991.
- [3] S. B. Seo, S. H. Lee, C. B. Yoon, G. T. Park, and H. E. Kim, "Low-temperature sintering and piezoelectric properties of 0.6Pb(Zr_{0.47}Ti_{0.53})O₃-0.4Pb(Zn_{1/3}Nb_{2/3})O₃ ceramics," *J. Am. Ceram. Soc.*, vol. 87, pp. 1238–1243, 2004.
- [4] Y. Yongke, K. Ashok, C. Margarita, C. Kyung-Hoon, R. S. Katiyar, and P. Shashank, *Applied Physics Letters*, vol. 100, pp. 152-902, 2012.
- [5] L. D. Vuong, P. D. Gio, T. V. Chuong, D. T. H. Trang, D. V. Hung, and N. T. Duong, "Effect of Zr/Ti ratio content on some physical properties of the low temperature sintering PZT-PZN-PMnN ceramics," *International Journal of Materials and Chemistry*, vol. 3, pp. 39-43, 2013.
- [6] L. D. Vuong and P. D. Gio, "Effect of Li₂CO₃ addition on the sintering behavior and physical properties of PZT-PZN-PMnN ceramics," *International Journal of Materials Science and Applications*, vol. 2, pp. 89-93, 2013.
- [7] F. Gao, L. Cheng, R. Hong, J. Liu, C. Wang, and C. Tian, "Crystal structure and piezoelectric properties of $x\text{Pb}(\text{Mn}_{1/3}\text{Nb}_{2/3})\text{O}_3-(0.2-x)\text{Pb}(\text{Zn}_{1/3}\text{Nb}_{2/3})\text{O}_3-0.8\text{Pb}(\text{Zr}_{0.52}\text{Ti}_{0.48})\text{O}_3$ ceramic," *Ceramics International*, vol. 35, pp. 1719–1723, 2009.
- [8] Y. H. Kim, H. Ryu, Y. K. Cho, H. J. Lee, and S. Nahm, "TEM observations on 0.65Pb(Zr_{0.42}Ti_{0.58})O₃-0.35Pb(Ni_{0.33}Nb_{0.67})O₃ Ceramics with CuO additive," *J. Am. Ceram. Soc.*, vol. 96, pp. 312–317, 2013.
- [9] M. K. Zhu, P. X. Lu, Y. D. Hou, H. Wang, and H. Yan, "Effects of Fe₂O₃ addition on microstructure and piezoelectric properties of 0.2PZN–0.8PZT ceramics," *J. Mater. Res.*, vol. 20, pp. 2670- 2675, 2005.
- [10] M. K. Zhu, P. X. Lu, Y. D. Hou, X. M. Song, H. Wang, and H. Yan, "Analysis of phase coexistence in Fe₂O₃ -Doped 0.2PZN–0.8PZT ferroelectric ceramics by raman scattering spectr," *J. Am. Ceram. Soc.*, vol. 89, pp. 3739–3744, 2006.
- [11] J. Li, H. Zhanbing, and D. Dragan, "Nanodomains in Fe³⁺-doped lead zirconate titanate ceramics at the morphotropic phase boundary do not correlate with high properties," *Applied Physics Letters*, vol. 95, p. 012905, 2009.

- [12] J. Du, J. Qiu, and K. Zhu, "Effects of Fe₂O₃ addition on microstructure and piezoelectric properties of 0.55Pb(Ni_{1/3}Nb_{2/3})–0.45Pb(Zr_{0.3}Ti_{0.7})O₃ ceramics," *J. Materials Letters*, vol. 66, pp. 507-510, 2012.
- [13] Y. D. Hou, L. M. Chang, M. K. Zhu, X. M. Song, and H. Yan, "Effect of Li₂CO₃ addition on the dielectric and piezoelectric responses in the low-temperature sintered 0.5PZN–0.5PZT systems," *Journal of Applied Physics*, vol. 102, p. 084507, 2007.
- [14] J. Frantti, Y. Fujioka, A. Poretzky, Y. Xie, and Z.-G. Ye, *J. Appl. Phys.*, vol. 113, p. 174104, 2013.
- [15] G. Burns, J. A. Sanjurjo, and E. Lopez-Cruz, "High-pressure raman study of two ferroelectric crystals closely related to PbTiO₃," *Phys. Rev. B*, vol. 30, p. 7170, 1984.
- [16] A. Sanjurjo, E. Lopez-Cruz, and G. Burns, *Solid State Comm.*, vol. 48, pp. 221–4, 1983.
- [17] G. Burns and B. A. Scott, "Lattice modes in ferroelectric perovskites: PbTiO₃," *Phys. Rev. B*, vol. 7, p. 3088, 1973.
- [18] B. Jaya Prakash and S. Buddhudu, *Indian Journal of Pure & Applied Physics*, vol. 50, pp. 320-324, 2012.
- [19] L. Ting, L. Junhong, D. Wenlong, X. Chenyang, and Z. Wendong, *Journal of Semiconductors*, vol. 30, 2009.
- [20] K. Uchino and S. Nomura, *Ferroelectr. Lett. Sect.*, vol. 44, p. 55, 1982.

Views and opinions expressed in this article are the views and opinions of the author(s), International Journal of Chemistry and Materials Research shall not be responsible or answerable for any loss, damage or liability etc. caused in relation to/arising out of the use of the content.